

Phase diagram of the spin- $\frac{3}{2}$ Blume-Capel model in three dimensions

S. Grollau

Laboratoire de Physique Théorique des Liquides, Université Pierre et Marie Curie, 4 Place Jussieu, 75252 Paris Cedex 05, France

(Received 29 January 2002; published 22 May 2002)

We use a thermodynamically self-consistent theory to obtain the phase diagram of the ferromagnetic spin- $\frac{3}{2}$ Blume-Capel model on the simple cubic lattice. The theory is based on an Ornstein-Zernike approximation where the direct correlation function is truncated and the dependence upon the thermodynamic variables is determined by a set of two coupled partial differential equations. Within this framework, we localize the critical line in zero external field with high accuracy and in good agreement with previous Monte Carlo analysis. At low temperature, in contrast with Monte Carlo results, we find a first-order transition line ending at a critical end point whose coordinates are given by $(k_B T_c / Jc = 0.213 \pm 0.003, \Delta_c / Jc = 0.491 \pm 0.001)$.

DOI: 10.1103/PhysRevE.65.056130

PACS number(s): 64.60.-i, 64.10.+h

I. INTRODUCTION

The spin- S Blume-Capel model is a generalization of the Ising model and is defined by the Hamiltonian

$$\mathcal{H} = -J \sum_{\langle ij \rangle} s_i s_j + \Delta \sum_i s_i^2 - h \sum_i s_i, \quad (1)$$

where $s_i = -S, -S+1, \dots, S$ is the spin variable at each site of a d -dimensional lattice and the first term sums over all nearest-neighbor pairs. The constant $J > 0$ defines the ferromagnetic exchange coupling, Δ is a single spin anisotropy parameter and h is an external field.

In the case where $S=1$, the Hamiltonian (1) defines the Blume-Capel model [1] and is a special case of the Blume-Emery-Griffiths (BEG) Hamiltonian [2], $\mathcal{H}_{BEG} = \mathcal{H} - K \sum_{\langle ij \rangle} s_i^2 s_j^2$, which represents a variety of interesting physical systems, in particular, ^3He - ^4He mixtures. The $S=1$ model has played an important role in the development of tricritical phenomena [3] and has been studied by a variety of methods such as the original mean-field treatment [1], series expansions [4], renormalization-group calculations [5,6], cluster-variation method [7], and Monte Carlo simulations [8]. The phase diagram of the Blume-Capel model is now well known and has been determined precisely for dimensions $d \geq 2$. It presents a line of second-order transitions (the so-called λ line) that separates the ferromagnetic ordered phase from the paramagnetic disordered phase. The transition line changes from second-order to first-order transitions at a tricritical point. Recently, two nonperturbative approaches, one based on a thermodynamically self-consistent theory [9] and the other one based on the momentum renormalization-group technique [10], have permitted to locate the coexistence curve in three dimensions with high accuracy, as well as the whole structure of the phase diagram including the “wing” boundaries in nonzero external field [9].

In the case where $S = \frac{3}{2}$, the model is a four-state spin model. Such models with additional terms in the Hamiltonian have been initially introduced to give a qualitative description of phase transitions observed in the compound DyVO_4 [11] and also to describe ternary mixtures [12]. In contrast to the case $S=1$, the phase diagram of the $S = \frac{3}{2}$ Blume-Capel is not well known and there are contradictions

among the available results. The mean-field treatment [13] that has been performed for the general Hamiltonian Eq. (1) predicts that the phase diagram differs for integer or half-odd-integer spins. More specifically, for $S = \frac{3}{2}$, the mean-field calculation indicates a line of second-order transitions for any value of Δ without the existence of a multicritical point, but with a line of first-order transitions at low temperature that ends up in an isolated critical end point. The results obtained for the phase diagram of the $S = \frac{3}{2}$ model in two dimensions have yielded to successive various conclusions. Whereas renormalization-group calculations [6,14] suggested the existence of a multicritical point, a recent study based on transfer matrix and conformal invariance [15] shows that there is no multicritical point in the phase diagram. In three dimensions, Monte Carlo simulations [16] for the simple cubic lattice suggest that the first-order transition line reaches the critical line, implying the existence of a multicritical point. Bethe-Peierls [17] and two-spin-cluster approximations [18] have been performed but neither of these studies explores the low-temperature region. On the other hand, a recent study obtained in the framework of two-spin-cluster approximation [19] that investigates the low-temperature region indicates a phase diagram in qualitative agreement with the mean-field prediction. However, this approach, as well as the mean-field analysis, overestimates the critical temperatures and does not locate the critical line with the same accuracy as the Monte Carlo predictions. In this context, one still needs an accurate and correct description of the phase diagram in three dimensions. The purpose of this paper is to study the $S = \frac{3}{2}$ Blume-Capel model using a thermodynamically self-consistent approach and to give a clear cut answer concerning the existence and the location of a critical end point. We believe that the phase diagram obtained in this study is the most precise in the present literature.

The approach used in this study is a self-consistent Ornstein-Zernike approximation (SCOZA) that has been introduced originally by Hoye and Stell [20] as a method for obtaining the thermodynamic and structural properties of simple fluids. This theory has then been developed and solved to study the lattice-gas model with nearest-neighbor attractive interactions [21] and more recently the Blume-Capel model [9]. Both studies show that this approach gives a very accurate description of the structural and thermody-

dynamic quantities even in the near vicinity of a critical point, yielding effective exponents close to the exact values. The transition temperature for second-order as well as first-order transition (see also the study of the Potts model [22]) are obtained with high accuracy compared to the best available estimates. This approach is based on the assumption that the direct correlation function $C(\mathbf{r})$ that is related to the two-particle distribution function $G(\mathbf{r})$ via the Ornstein-Zernike equation has always the same range as the pair potential. In the case of the lattice gas, the dependence on the thermodynamic variables giving $C(\mathbf{r})$ uniquely is determined first from a partial differential equation, which ensures that the same free energy is obtained from fluctuation theory or the so-called compressibility route and from integration of the internal energy with respect to the inverse temperature, and second from the requirement of single site occupancy. In the case of the Blume-Capel model, $C(\mathbf{r})$ is obtained as the solution of two coupled partial differential equations that ensure the thermodynamical self-consistency. The paper is organized as follows. In Sec. II, we present the theory for the $S = \frac{3}{2}$ Blume-Capel model. In Sec. III, we give the phase diagram in zero external field and we compare our results with previous analyses.

II. THEORY

Our theory is based on an Ornstein-Zernike approximation for the direct correlation function C_{ij} , where C_{ij} is related to the connected pair correlation function $G_{ij} = \langle S_i S_j \rangle - \langle S_i \rangle \langle S_j \rangle$ via the Ornstein-Zernike (OZ) equations

$$\sum_k G_{ik} C_{kj} = \delta_{ij}, \quad (2)$$

where δ_{ij} is the Kronecker symbol. The OZ equation is a consequence of the Legendre transform

$$\mathcal{G}(T, \Delta, \{m_i\}) = \mathcal{F}(T, \Delta, \{h_i\}) + \sum_i h_i m_i \quad (3)$$

that defines the Gibbs free energy \mathcal{G} from the free energy $\mathcal{F} = -k_B T \ln \text{Tr} \exp[-\mathcal{H}/k_B T]$. The free energy \mathcal{F} is a function of the inverse temperature $\beta = 1/k_B T$, the single spin anisotropy parameter Δ and the site dependent magnetic field h_i , whereas the Gibbs free energy \mathcal{G} is a function of β , Δ and the local magnetization m_i . The connected and direct correlation functions are obtained as the second derivatives of \mathcal{F} and \mathcal{G} with respect to the local field and local magnetization

$$G_{ij} = - \frac{\partial^2 \tilde{\mathcal{F}}}{\partial \tilde{h}_i \partial \tilde{h}_j}, \quad (4)$$

$$C_{ij} = \frac{\partial^2 \tilde{\mathcal{G}}}{\partial m_i \partial m_j}, \quad (5)$$

where $\tilde{\mathcal{F}} = \beta \mathcal{F}$, $\tilde{\mathcal{G}} = \beta \mathcal{G}$, and $\tilde{h}_i = \beta h_i$. In the case of a uniform magnetic field $h_i = h$ (or equivalently for $m_i = m$), the system is translationally invariant and the correlation func-

tions $C(\mathbf{r})$ and $G(\mathbf{r})$ depend only on the vector \mathbf{r} that connects the two sites. In general, the direct correlation function $C(\mathbf{r})$ is expected to remain of finite range, even at the critical point [23]. Following the OZ approximation, we assume here that $C(\mathbf{r})$ has exactly the range of the exchange interaction in the Hamiltonian Eq.(1). This assumption implies that $C(\mathbf{r})$ is truncated at nearest-neighbor (NN) separation and we thus write

$$C(\mathbf{r}) = c_0(\tilde{\mathcal{J}}, \tilde{\Delta}, m) \delta_{\mathbf{r},0} + c_1(\tilde{\mathcal{J}}, \tilde{\Delta}, m) \delta_{\mathbf{r},\mathbf{e}} \quad (6)$$

where \mathbf{e} denotes a vector from the origin to one of its NN, c_0 and c_1 are two arbitrary functions that depend on the thermodynamic variables $\tilde{\mathcal{J}} = \beta J$, $\tilde{\Delta} = \beta \Delta$, and m . As is well known in liquid-state theory [23], when one assumes some approximate but explicit dependence of the direct correlation function upon the thermodynamic variables, as in the random phase approximation or in the mean-spherical approximation, the theory is in general thermodynamically inconsistent. In our self-consistent approach, the assumption Eq. (6) is the *only* approximation of the theory and the two functions c_0 and c_1 are determined by imposing the thermodynamic consistency, as explained below.

One consequence of the assumption Eq. (6) is that the two-point correlation function is given by

$$G(\mathbf{r}) = \frac{1}{c_0} P(\mathbf{r}, z), \quad (7)$$

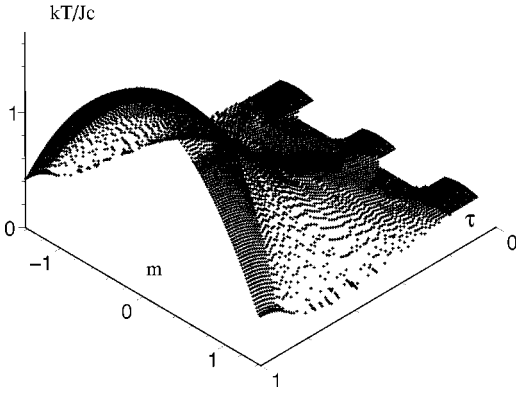
where

$$P(\mathbf{r}, z) = \frac{1}{(2\pi)^d} \int_{-\pi}^{\pi} d\mathbf{k} \frac{e^{-i\mathbf{k} \cdot \mathbf{r}}}{1 - z \hat{\lambda}(\mathbf{k})} \quad (8)$$

is the lattice Green's function. In the Eqs. (7) and (8), we have introduced the characteristic function of the lattice $\lambda(\mathbf{k}) = (1/c) \sum_{\mathbf{e}} e^{i\mathbf{k} \cdot \mathbf{e}}$ and we have substituted the unknown function c_1 with the new one $z = -(c_1/c_0)c$, where c is the coordination number. The expression Eq. (7) of $G(\mathbf{r})$ implies that the exponent η giving the asymptotic behavior of $G(\mathbf{r})$ at the critical point [$G(\mathbf{r}) \sim C/r^{d-2+\eta}$] is equal to zero. However, an important feature of the SCOZA is that the other exponents do not take necessarily classical or spherical values. In particular, the spontaneous magnetization for the Ising model is accurately described with the exponent $\beta = 0.35$ [24] (see also Refs. [9] and [21] for the critical properties of SCOZA).

In a previous work, the SCOZA equations have been derived for the Blume-Capel model [9]. In that case, thermodynamic consistency is encoded in two partial differential equations. These two equations [Eqs. (16a) and (16b) of that reference] are in fact valid for the most general Hamiltonian Eq. (1). To derive these equations, one considers the change in the free energy associated with infinitesimal changes in $\tilde{\mathcal{J}}$, $\tilde{\Delta}$, and \tilde{h} :

$$\delta \tilde{\mathcal{F}} = -\delta \tilde{\mathcal{J}} \sum_{\langle ij \rangle} \langle S_i S_j \rangle + \delta \tilde{\Delta} \sum_i \langle S_i^2 \rangle - \delta \tilde{h} \sum_i \langle S_i \rangle. \quad (9)$$


 FIG. 1. SCOZA spinodal surface in the $(T-\tau-m)$ space.

In terms of the pair-correlation function, the corresponding change in the Gibbs free energy is given by

$$\delta\tilde{\mathcal{G}}/N = -\frac{1}{2} [G(\mathbf{r}=\mathbf{e}) + m^2] \delta\lambda + [G(\mathbf{r}=\mathbf{0}) + m^2] \delta\tilde{\Delta} + \tilde{h} \delta m, \quad (10)$$

where N is the number of lattice sites and $\lambda = c\tilde{J}$.

For the theory to be thermodynamically consistent, the Gibbs potential $\tilde{\mathcal{G}}$ must have the same value when integrating with respect to λ , $\tilde{\Delta}$, or m . This thermodynamic consistency is embodied in two independent Maxwell relations between the partial derivatives of $\tilde{\mathcal{G}}$ with respect to the control variables (see [9] for a detailed derivation of these equations):

$$\frac{\partial \hat{C}(\mathbf{k}=\mathbf{0})}{\partial \lambda} = -\frac{1}{2} \frac{\partial^2}{\partial m^2} [G(\mathbf{r}=\mathbf{e}) + m^2], \quad (11)$$

$$\frac{\partial G(\mathbf{r}=\mathbf{0})}{\partial \lambda} = -\frac{1}{2} \frac{\partial G(\mathbf{r}=\mathbf{e})}{\partial \tilde{\Delta}}. \quad (12)$$

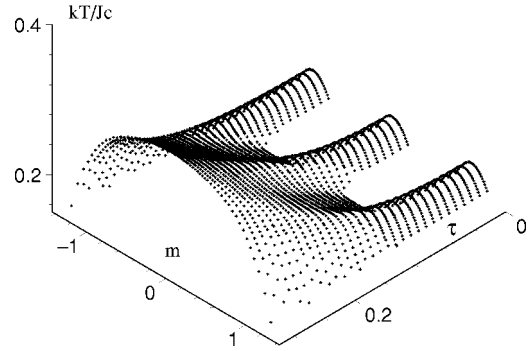
Using the expression of the correlation functions, Eqs. (6) and (7), one obtains the two SCOZA equations

$$\frac{\partial}{\partial \lambda} c_0(1-z) = -1 - \frac{1}{2} \frac{\partial^2}{\partial m^2} \frac{P(z)-1}{zc_0}, \quad (13)$$

$$\frac{\partial}{\partial \lambda} \frac{P(z)}{c_0} = \frac{1}{2} \tau(1-\tau) \frac{\partial}{\partial \tau} \frac{P(z)-1}{zc_0}, \quad (14)$$

where $\tau = (1 + \frac{1}{2} e^{\tilde{\Delta}})^{-1}$ varies from 0 to 1 and $P(z) = P(z, \mathbf{r}=\mathbf{0})$. Finally, for the theory to be completely defined, one has to determine the appropriate boundary conditions for the solution to the Eqs. (13) and (14).

The full range of variation of the inverse temperature λ is from 0 to ∞ and that of the magnetization m goes from $-\frac{3}{2}$ to $\frac{3}{2}$ (because of the symmetry $m \rightarrow -m$, one can restrict the domain to $m \geq 0$). $\lambda=0$ corresponds to the initial condition provided by the exact solution of the noninteracting model in an external field. For this system, the correlation functions are nonzero only at $\mathbf{r}=\mathbf{0}$ that implies that $z=0$. From the spontaneous magnetization


 FIG. 2. Detail of the spinodal surface in the region $0.28 \leq \tau \leq 0$.

$$m = \frac{1}{2} \frac{(x-1)(3x^2+x(3+u)+3)}{(x+1)(x^2+x(u-1)+1)}, \quad (15)$$

where $x = e^{\tilde{h}}$ and $u = 4(1-\tau)^2/\tau^2$, one obtains

$$\begin{aligned} c_0 = \hat{C}(\mathbf{k}=\mathbf{0}) &= \frac{\partial^2 \tilde{\mathcal{G}}/N}{\partial m^2} = (k_B T \chi^{-1}) \\ &= \frac{(1+x)^2 [x^2 + x(u-1) + 1]^2}{x [ux^4 + 4ux^3 + x^2(u^2+9) + 4ux + u]}. \end{aligned} \quad (16)$$

The boundary condition $m = \frac{3}{2}$ corresponds also to a trivial system where in that case all the spins are in the $S = \frac{3}{2}$ state. For $m = \frac{3}{2}$, one has $z=0$, and $G(\mathbf{r}=\mathbf{0}) = \frac{9}{4} - m^2 = P(z)/c_0$ implies that $P(z)/c_0 = 0$ (or $c_0 \rightarrow \infty$).

Finally, one has to determine the functions z and c_0 for $\tau=1$ and $\tau=0$. Inserting $\tau=1$ in Eq. (14) leads to the fact that $P(z)/c_0 = f(m)$ is a function of m independent of λ .

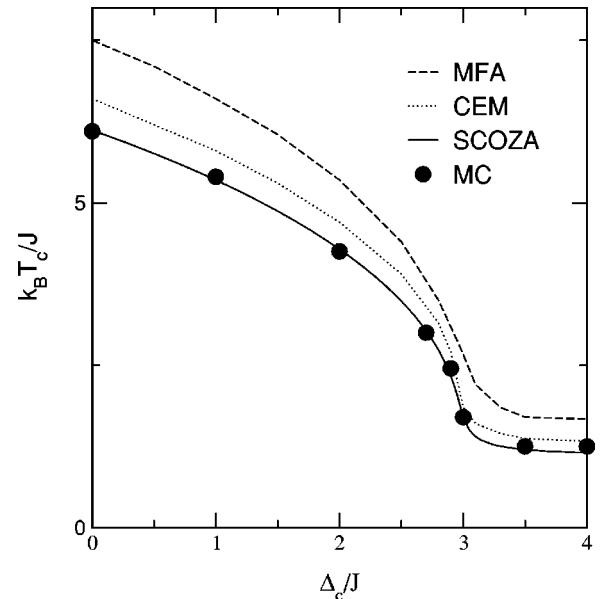


FIG. 3. Critical line in zero external field. The SCOZA results are compared those obtained with the mean-field approximation (MFA) [13], the cluster expansion method (CEM) [19] and Monte Carlo simulation (MC) [16].

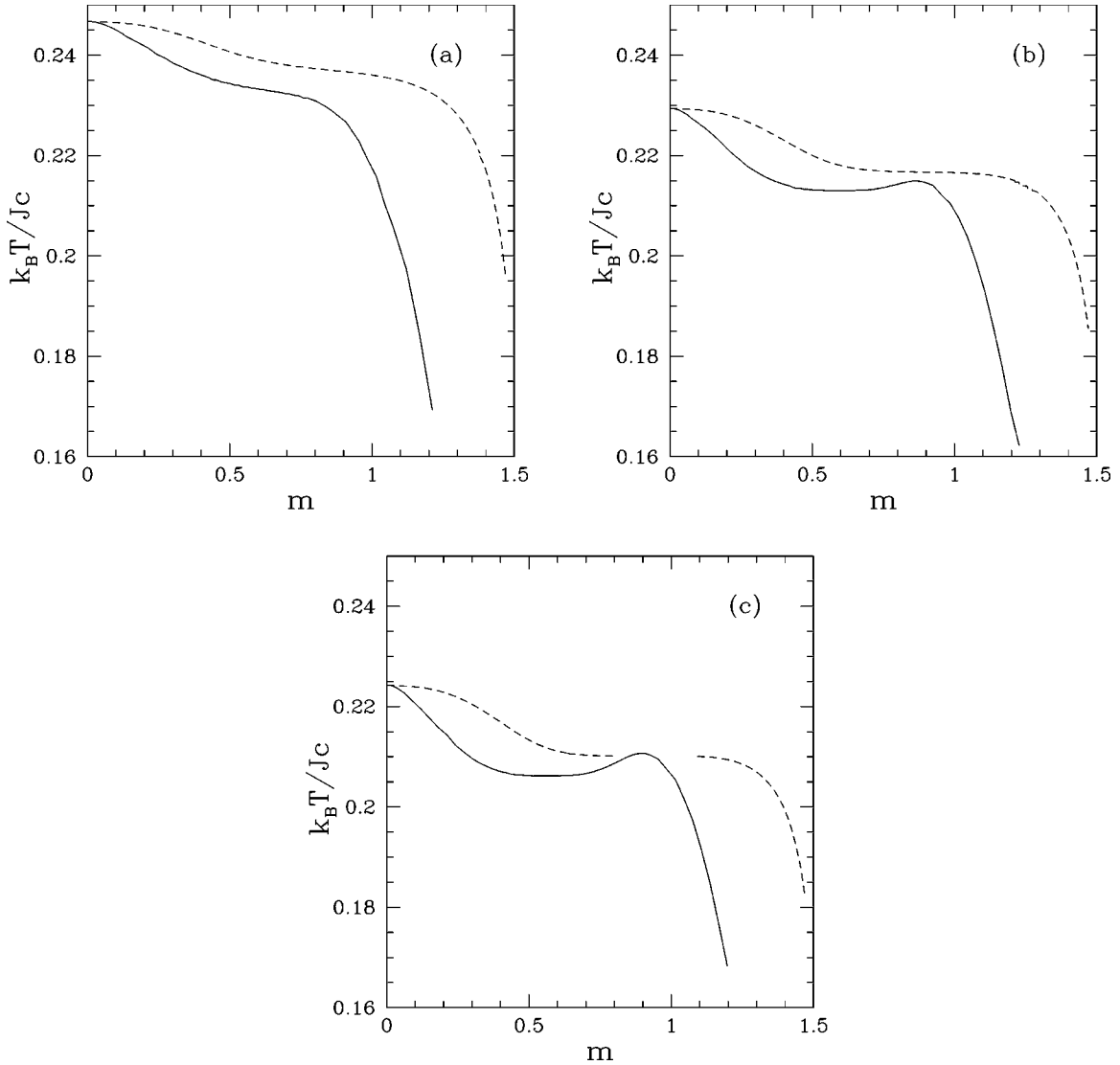


FIG. 4. Spontaneous magnetization (dashed lines) and spinodal curves (full lines) vs temperature for $\tau=0.20$ (a), $\tau=0.17$ (b), and $\tau=0.16$ (c).

This function $f(m)$ may be determined for the system without interaction, $\lambda=0$. By inserting $\tau=1$ in Eq. (16), one obtains $f(m)=\frac{9}{4}-m^2$. The equation for the remaining variable $z(\lambda, m)$ becomes

$$\frac{1}{\frac{9}{4}-m^2} \frac{\partial}{\partial \lambda} (1-z)P(z) = -1 - \frac{1}{2} \frac{\partial^2}{\partial m^2} \left[\left(\frac{9}{4} - m^2 \right) \frac{P(z)-1}{zP(z)} \right], \quad (17)$$

which is nothing else than the SCOZA equation for the Ising model where the spins assume the values $\pm \frac{3}{2}$. Indeed, the boundary condition $\tau=1$ corresponds to the limit $\Delta \rightarrow -\infty$ where in that case all the states $S = \pm \frac{1}{2}$ are suppressed.

One obtains in a similar way the boundary condition for $\tau=0$. In that case, the variable $z(\lambda, m)$ is determined by the solution of the equation

$$\frac{1}{f(m)} \frac{\partial}{\partial \lambda} (1-z)P(z) = -1 - \frac{1}{2} \frac{\partial^2}{\partial m^2} \left[f(m) \frac{P(z)-1}{zP(z)} \right], \quad (18)$$

where $f(m)=\frac{1}{4}-m^2$ for $0 \leq m \leq \frac{1}{2}$ and $f(m)=(m-\frac{1}{2})(\frac{3}{2}-m)$ for $m \geq \frac{1}{2}$. $\tau=0$ corresponds to the limit $\Delta \rightarrow +\infty$. In this limit and for a finite external field h , the states $S = \pm \frac{3}{2}$ are suppressed and the solution of Eq. (18) on the domain $0 \leq m \leq \frac{1}{2}$ corresponds to the SCOZA equation for the $S = \pm \frac{1}{2}$ Ising model. On the other hand, for an infinite external field, the states $S = \pm \frac{3}{2}$ may be populated. The solution of Eq. (18) on the domain $\frac{1}{2} \leq m \leq \frac{3}{2}$ corresponds to this limit $h \rightarrow +\infty$. In particular, it gives the location of the critical point marking the end of the wing critical line (this critical wing is the critical line that separates the two phases where either the $S = \frac{1}{2}$ or the $S = \frac{3}{2}$ spin states are populated).

Thus, Eqs. (13) and (14) with the above boundary conditions define the SCOZA theory for the $S = \frac{3}{2}$ Blume-Capel

model. We have performed the numerical resolution of these equations, (13) and (14), with an explicit algorithm where the partial derivatives are approximated by finite difference representations. From the initial condition $\lambda=0$, the finite representation of Eqs. (14) and (15) gives the functions c_0 and z at the next step in the λ direction, $\lambda = \delta\lambda$. Once c_0 and z are known at the inverse temperature λ , the same procedure is repeated to obtain c_0 and z at the new step $\lambda + \delta\lambda$. To ensure the numerical stability of the explicit scheme, $\delta\lambda$ is gradually decreased as the spinodal is approached, the spinodal being defined by the divergence of the susceptibility $k_B T \chi$. The shape and the localization of the spinodal is not known *a priori* but given by the numerical resolution and it defines the lower bound of the domain of definition of the Eqs. (13) and (14). During the numerical procedure, we integrate the Gibbs free energy

$$\frac{\tilde{\mathcal{G}}}{N}(\lambda, \tilde{\Delta}, m) = \int_0^\lambda -\frac{1}{2}[G(\mathbf{r}=\mathbf{e}) + m^2] \delta\lambda + \frac{\tilde{\mathcal{G}}}{N}(\lambda=0, \tilde{\Delta}, m), \quad (19)$$

where $G(\mathbf{r}=\mathbf{e}) = (1-m^2)[P(z) - 1/zP(z)]$ and $\tilde{\mathcal{G}}(\lambda=0, \tilde{\Delta}, m)$ is the Gibbs free energy for the system without interaction. In the following section, we present the results obtained for the phase diagram in zero external field, $h=0$. In the disordered phase, the zero field solution is given by the Gibbs free energy at $m=0$ whereas in the ordered phase, the zero field solution and in particular the spontaneous magnetization is obtained from the condition $h(T, m) = (\partial\mathcal{G})/(\partial m) = 0$.

III. RESULTS AND DISCUSSION

We have performed the numerical resolution for the simple cubic lattice using the corresponding integral expression of the lattice Green's function [25].

The global shape of the spinodal in space (T, m, τ) and the details for small values of τ are depicted in Figs. 1 and 2, respectively. For a fixed value of τ , the spinodal in the T - m plane presents a maximum at $m=0$. This maximum corresponds to a critical point in zero external field. For small value of τ , the spinodal in the T - m plane presents three distinct maxima. The two symmetric maxima with respect to the plane $m=0$ correspond to the two critical points in external field (points of the two symmetrical critical wings).

The critical line in zero external field is represented in Fig 3 in the T - Δ plane. We obtain the critical temperatures for the $S = \pm \frac{3}{2}$ ($\tau=1$) and for the $S = \pm \frac{1}{2}$ ($\tau=0$) Ising model, $9\tilde{J}_c = 0.88489$ and $\tilde{J}_c = 0.88478$, respectively. These values are in perfect agreement with that obtained in Ref. [21] and they are within 0.2% of the best estimate for the Ising model (see [21] and references therein). We believe that the SCOZA predictions for the critical temperatures in the whole range of the values of the crystal field Δ are obtained with the same accuracy as the one obtained for the two limits $\tau=0$ and $\tau=1$. We have reported on the Fig 3 the results obtained with the mean-field approximation (MFA) [13], with a cluster expansion method (CEM) [19] and results from Monte Carlo

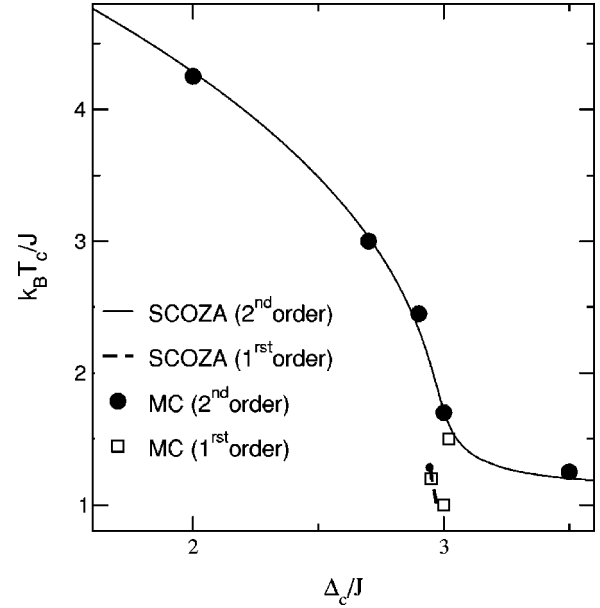


FIG. 5. Phase diagram in the neighborhood of the critical end point. Monte Carlo (MC) results suggest a first-order transition line reaching the critical line. The SCOZA results give a critical end point (small circle).

simulations (MC) [16]. This comparison shows how the estimates of the critical temperature decrease when the effect of fluctuations is taken into account. The CEM gives a significant correction to the mean-field prediction and SCOZA brings additional corrections yielding a very good agreement with the Monte Carlo predictions.

We have calculated the spontaneous magnetization curves for several values of τ . In Fig. 4, the spinodal and the spontaneous magnetization curves are represented in the plane T - m for three values of τ , $\tau=0.20$, $\tau=0.17$, and $\tau=0.16$. We observe that for $\tau=0.20$, the spontaneous magnetization decreases continuously as the temperature decreases, with a curve located well above the spinodal curve. For $\tau=0.17$, the spontaneous magnetization curve is still continuous, but becomes close to the spinodal curve for a nonzero value of the magnetization. For $\tau=0.16$, the spontaneous magnetization curve presents a discontinuity at the temperature $k_B T_c / J_c \approx 0.21$. This discontinuity corresponds to the first-order transition at low temperature. Between the two values $\tau=0.16$ and $\tau=0.17$, there is a critical value τ_c for which the spontaneous magnetization is tangent to the spinodal at a nonzero value of m . This value τ_c corresponds to the critical value of the coordinates of the critical end point marking the end of the first-order transition line. To obtain more precisely the coordinates of the critical end point, we decrease the mesh division of the grid in the numerical procedure. We thus have found that the coordinates of the critical end point are $k_B T_c / J_c = 0.213(3)$, $\Delta_c / J_c = 0.491(1)$, and $\tau_c = 0.167(5)$. This value of Δ_c / J_c is close to the CEM value ($\Delta_c^{CEM} / J_c \approx 0.49225$) whereas the mean-field value is slightly lower ($\Delta_c^{MFA} / J_c \approx 0.486$). These two methods however overestimate significantly the critical temperature with $k_B T_c^{MFA} / J_c \approx 0.3$ and $k_B T_c^{CEM} / J_c \approx 0.2327$.

Finally, the critical line and the first-order transition line in the neighborhood of the critical end point are depicted in Fig. 5 in the T - Δ plane. We have reported on this figure the MC results. The SCOZA predictions give a critical end point very close to but below the critical line. The phase diagram is thus in qualitative agreement with the mean-field predictions. The agreement between the SCOZA and the simulations is very good for the whole phase diagram including the critical line as well as the first-order one. However, the simulations indicate a point of first-order transition that suggests that the first-order transition line reaches the critical one. According to the accuracy of the SCOZA to locate first-order as well as second-order transition, we believe that the SCOZA gives the correct phase diagram. The first-order transition line ends up in an isolated critical point and there is no multicritical point in the phase diagram of the three-dimensional $S = \frac{3}{2}$ Blume-Capel model.

IV. CONCLUSION

In this paper, we have obtained the phase diagram of the three-dimensional $S = \frac{3}{2}$ Blume-Capel model using a thermo-

dynamically self-consistent theory. This approach allows us to locate first-order and second-order transitions with high accuracy. The critical line as well as the first-order transition line compared very well with the Monte Carlo predictions. Besides, different from the Monte Carlo results, the SCOZA is accurate enough to obtain the coordinates of the critical end point that terminates the first-order transition line and that is located just below the critical line. We thus obtain a phase diagram in qualitative agreement with the mean-field prediction. This work as well as previous studies show that the SCOZA is a powerful tool to study three dimensional spin model and that the predictions for nonuniversal quantities such as the critical temperatures can be considered as faithful estimates.

ACKNOWLEDGMENTS

The author is grateful to M.L. Rosinberg and to G. Tarjus for many fruitful discussions.

-
- [1] M. Blume, Phys. Rev. **141**, 517 (1966); H.W. Capel, Physica (Amsterdam) **32**, 966 (1966).
 - [2] M. Blume, V.J. Emery, and R.B. Griffiths, Phys. Rev. A **4**, 1071 (1971).
 - [3] I.D. Lawrie and S. Sarbach, in *Phase Transitions and Critical Phenomena*, edited by C. Domb and J. L. Lebowitz (Academic, London, 1984), Vol 9.
 - [4] P.F. Fox and D.S. Gaunt, J. Phys. C **5**, 3085 (1972); Oitmaa, *ibid.* **5**, 435 (1972); D.M. Saul, M. Wortis, and D. Stauffer, Phys. Rev. B **9**, 4964 (1974).
 - [5] A.N. Berker and M. Wortis, Phys. Rev. B **14**, 4946 (1976); G.D. Mahan and S.M. Girvin, *ibid.* **17**, 4411 (1978); O.F. de Alcântara Bonfim, Physica A **130**, 367 (1985).
 - [6] P.M.C. de Oliveira, Europhys. Lett. **20**, 621 (1992); S.M. de Oliveira, P.M.C. de Oliveira, and F.C. de SáBarreto, J. Stat. Phys. **78**, 1619 (1995).
 - [7] S.L. Lock and B.S. Lee, Phys. Status Solidi B **124**, 593 (1984).
 - [8] A.K. Jain and D.P. Landau, Phys. Rev. B **22**, 445 (1980); M. Deserno, Phys. Rev. E **56**, 5204 (1997).
 - [9] S. Grollau, E. Kierlik, M.L. Rosinberg, and G. Tarjus, Phys. Rev. E **63**, 041111 (2001).
 - [10] A. Brognara, A. Parola, and L. Reatto, Phys. Rev. E (to be published).
 - [11] J. Sivardière and M. Blume, Phys. Rev. B **5**, 1126 (1972).
 - [12] S. Krinsky and D. Mukamel, Phys. Rev. B **11**, 399 (1975).
 - [13] J.A. Plascak, J.G. Moreira, and F.C. Sá Barreto, Phys. Lett. A **173**, 360 (1993).
 - [14] A. Bakchich, A. Bassir, and A. Benyoussef, Physica A **195**, 188 (1993).
 - [15] J.C. Xavier, F.C. Alcaraz, D. Penna Lara, and J.A. Plascak, Phys. Rev. B **57**, 11 575 (1998).
 - [16] F.C. de Sá Barreto and O.F. de Alcântara Bonfim, Physica A **172**, 378 (1991).
 - [17] T. Kaneyoshi, J.W. Tucker, and M. Jascur, Physica A **186**, 495 (1992); G. Le Gal, T. Kaneyoshi, and A. Khater, *ibid.* **195**, 174 (1993).
 - [18] M. Jurcisin, A. Bobak, and M. Jascur, Physica A **224**, 684 (1996).
 - [19] V. Ilkovic, Physica A **234**, 545 (1996).
 - [20] J.S. Hoye and G. Stell, J. Chem. Phys. **67**, 439 (1977); Mol. Phys. **52**, 1071 (1984); Int. J. Thermophys. **6**, 561 (1985).
 - [21] R. Dickman and G. Stell, Phys. Rev. Lett. **77**, 996 (1996); D. Pini, G. Stell, and R. Dickman, Photonics Spectra **57**, 2862 (1998).
 - [22] S. Grollau, M.L. Rosinberg, and G. Tarjus, Physica A **296**, 460 (2001).
 - [23] J. P. Hansen and I. R. McDonald, *Theory of Simple Liquids* (Academic Press, New York, 1976).
 - [24] J.S. Hoye, D. Pini, and G. Stell, Physica A **279**, 213 (2000).
 - [25] G.S. Joyce, J. Phys. C **4**, L53 (1971).